Applying different angular ordering constraints and k_t-factorization approaches to the single inclusive hadron production in the e^+e^- annihilation processes

M. Modarres* and R. Taghavi

Department of Physics, University of Tehran, 1439955961 Tehran, Iran

(Received 6 July 2021; accepted 9 November 2021; published 3 December 2021)

We study the differential cross section of the single inclusive e^+e^- annihilation to the hadrons via γ-production, in the different k_t-factorization frameworks. In order to take into account the transverse momenta of the incoming partons, for the first time, we apply the Kimber *et al.* (KMR) method to calculate the unintegrated parton fragmentation functions (UFFs) from the ordinary integrated one, i.e., the parton fragmentation functions (FFs), which satisfy the similar Dokshitzer-Gribov-Lipatov-Altarelli-Parisi (DGLAP) evolution equations, such as those of parton distribution functions (PDFs). Also, by utilizing the different angular ordering constraints the results corresponding to the Martin *et al.* (MRW) in the leading order (LO) and the next-to-leading-order (NLO) are obtained. The LO sets of DSS library for the input FFs is used. The numerical results are compared with the experimental data in the different energies which are reported by the different collaborations, such as TASSO, AMY, MARK II, CELLO, DELPHI, SLD, ALEPH and Belle with the other QCD + fragmentation models such as PYTHIA6.4 and 8.2 parton showers. The behaviors of the normalized differential cross sections and the multiplicity versus the "transverse momentum" ($p_\perp$) are discussed. The final results demonstrate that the KMR and MRW UFFs give a good description of data and there is not much significant difference between the above three schemes. On the other hand, our results become closer to the data for the lower values of $p_\perp$ and the higher values of center of mass energies.

DOI: 10.1103/PhysRevD.104.114004

I. INTRODUCTION

The discovery of the partonic structure of hadrons based on quarks and gluons is one of the most interesting topics in the theoretical and experimental high energy physics. The parton distribution functions (PDFs) represent the densities of these fundamental particles which initially depend on the Bjorken variable x and the hard scale μ^2 by Dokshitzer-Gribov-Lipatov-Altarelli-Parisi (DGLAP) evolution equations [1–4]. However, the experimental data of hadron-hadron colliders show that the significant information is embedded in the transverse momentum of the initial hadron constituents. So the important inputs are the unintegrated parton distribution functions (UPDFs). The UPDFs can be interpreted as number densities of partons that are carrying a fraction x of the momentum of parent hadron with the transverse momentum k_t at the hard scale μ^2. These transverse dependent functions extensively were investigated in the Drell-Yan and the semi-inclusive deep inelastic scattering (SIDIS) processes and unlike the collinear ones, they are still highly debated subjects [5–7]. Theoretically, various methods are utilized to generate these fundamental quantities, and among them, the Kimber *et al.* [8] and Martin *et al.* [9] formalisms are more simplistic ways to describe these UPDFs. The general behavior of these prescriptions was investigated in Refs. [10–14].

Of equal importance is the hadronization mechanism of the generation of mesons and baryons from partons. To reach a comprehensive description of these processes the fragmentation functions (FFs) are required [15–19]. These nonperturbative fundamental quantities mean the probability of carrying the light-cone fraction z of the fragmenting parent parton by hadron H, and can be measured in SIDIS and single- or double-inclusive hadron production in the electron-positron annihilation processes. While FFs are necessarily coupled to the PDFs in SIDIS, the single inclusive annihilation provides a golden channel and a cleanest electromagnetic probe to study FFs, because there is no contribution from hadronic effects in the initial states [20]. At the first order and c.m. energies below the Z^0 mass, this process can be interpreted as $e^+e^- \to HX$, via a single

*Corresponding author.
mmodares@ut.ac.ir

virtual photon, which can subsequently fragment into the hadrons (H). The direction of the fragmenting back to back $q\bar{q}$ pair is identified by the jet axis resulting from each e^+e^- scattering, and the detected $p_\perp$ represents a direct measurement of the transverse momentum of the final hadron with respect to the fragmenting parent parton.

Some data upon polarized Collins FFs were achieved by the *BABAR* collaboration [21,22] and some literature on this subject is presented [23–25]. But, a little experimental information exists on the unpolarized transverse momentum dependent FFs. Although a thorough knowledge of these functions would be of fundamental importance for studying the transverse motion of hadrons, because of lack of data on $p_\perp$ distribution of e^+e^- unpolarized cross sections, limited studies were performed over these functions [26–34]. However, in this paper, we concentrate on the data for single-inclusive hadron cross section in the e^+e^- annihilation process, $e^+e^- \to HX$, from the TASSO collaboration at PETRA (DESY) [35,36]. The advantage of these datasets, which are integrated over z with a small average value of z_H, $\langle z_H \rangle$, is delivering measurements at the different c.m. energies. They provide the differential cross sections in terms of $p_\perp$, normalized to the fully inclusive cross section which has interesting features to be studied under the k_t-factorization scheme. In this work, the cross section data as a function of $p_\perp$ distributions, integrated over the energy fraction z of the detected hadron H, for all charged particles production in the different c.m. energies between 14 and 44 GeV are considered. Moreover, we also consider the MARKII [37], AMY [38] and CELLO [39] collaboration data collected at the SLAC storage ring PEP, the KEK collider TRISTAN and at the PETRA, respectively. Also, the e^+e^- unpolarized cross sections are discussed for PYTHIA6.4 and PYTHIA8.2 parton showers [40] in comparison with those of DELPHI [41], SLD [42] and ALEPH [43] collaborations data at c.m. energy 91 GeV.

Although these data are old and limited to the $p_\perp$ distribution, they represent extremely valuable and unique information of a direct measurement of intrinsic transverse momenta of the final hadrons with respect to the fragmented parent parton. These data in the nonperturbative region, $p_\perp < 1$ GeV, are phenomenologically studied by Boglione *et al.* [31–33], considering two functional forms, i.e., the Gaussian and the power law, as models for fitting to reproduce the behavior of data at small $p_\perp$. There is also the newer data from the Belle collaboration [44]. These data provide the unpolarized cross sections of charged pions and kaons based on z, $p_\perp$ and event shape variable $(d^3\sigma/dzdp_\perp dT)$ in the $\sqrt{s} = 10.58$ GeV Belle collaboration [44]. In these datasets the transverse momentum of the produced hadron is calculated relative to the thrust axis $\hat{\mathbf{n}}$ which maximizes the event-shape variable thrust T:

$$T \overset{\max}{=} \frac{\sum_h |\mathbf{P}_h^{\text{c.m.system}} \cdot \hat{\mathbf{n}}|}{\sum_h |\mathbf{P}_h^{\text{c.m.system}}|},$$

in which the sum runs over all detected particles, and the momentum of hadron h in the c.m. system, denoted by $P_h^{\text{c.m.system}}$. It is shown in Ref. [44] that uds and charm events have a peak at high thrust values. That is why in this work, our results will be displayed in the $0.85 < T < 0.9$ thrust bin. We also select high z bin datasets, because our perturbative formalisms are valid for $p_\perp > 1$ GeV.

In this work, we intend to constrain our analysis to the region of $p_\perp > 1$ GeV in which there are perturbative effects. We apply, for the first time, the Kimber *et al.* (KMR) and Martin *et al.* (MRW) formalisms in the leading and next-to-leading order to test the capability of these procedures in obtaining the unintegrated parton fragmentation functions (UFFs), $D(z, p_\perp, \mu^2)$. It is essential to emphasize that our goal here is not so much the determination of UFFs, which would require all possible processes, but rather to explore, the application of the KMR and MRW methodology for finding UFFs. So, we restrict ourselves to the lowest order of QCD, and neglect all terms related to $\alpha_s(\mu^2)$ in the differential cross section calculations.

The results are compared with distributions generated by QCD + fragmentation model programs via Monte Carlo techniques such as the leading-logarithmic parton shower (Lund PS) [45], the second-order matrix-element calculation (Lund ME) [46], and the model of the Gottschalk and Morris (CALTECH II) [47] at the parton level. The main approach of all these programs is utilizing a model with a few free parameters in the fitting to the data processes. The important features of these models are briefly discussed in Refs. [37,38]. Beside these parton showers, there is also the possibility of comparison of the result with those of PYTHIA6.4 and PYTHIA8.2 [40].

The organization of our paper is as follows: In Sec. II, we review briefly the basic formulas of the cross section of e^+e^- annihilation into hadrons, k_t-factorization approach, and the KMR methodology to construct the UPDFs and UFFs. In Sec. III we present the numerical results and discussions. Finally, we summarize our conclusions in Sec. IV.

II. THE FORMALISM

A. The cross section and the fragmentation functions

In this section, we present some theoretical aspects of the cross section of the single inclusive hadron production in the e^+e^- annihilation process into a single hadron H,

$$e^+e^- \to \gamma \to HX, \tag{1}$$

by considering unpolarized fragmentation function. The cross section for such a process by including the transverse momentum can be typically written in the following form:

$$\frac{1}{\sigma_{\rm tot}}\frac{d\sigma^H}{dzd^2\vec{p}_\perp}=\frac{1}{\sum_q {e_q}^2}[2F_1^H(z,p_\perp;\mu^2)+F_L^H(z,p_\perp;\mu^2)], \tag{2}$$

where e_q is the charge of each quark flavor and the sum runs over all active quark-antiquark flavors. The energy E_H of fragmented hadron with respect to the beam energy $\frac{\sqrt{s}}{2}$ is presented by the parameter $z=2p_H.q/\mu^2=2E_H/\sqrt{s}$ which, in the e^+e^- c.m. frame, is interpreted as the momentum fraction of the parent quark carried by the produced hadron. Details on the unpolarized timelike structure functions F_1^H and F_L^H in Eq. (2) can be found in Refs. [48,49]. The total cross section for the e^+e^- annihilation to hadrons is presented by

$$\sigma_{\rm tot}(\mu^2)=\sum_q {e_q}^2\sigma_0\left[1+\frac{\alpha_s(\mu^2)}{\pi}\right]+\mathcal{O}(\alpha_s^2), \tag{3}$$

where $\sigma_0=\frac{4\pi\alpha^2}{3s}$ in which $\alpha=e^2/4\pi$ denotes the electromagnetic fine structure constant, and in the leading order in α_s, we have $\sigma_{\rm tot}=\frac{4\pi\alpha^2}{3s}\sum_q {e_q}^2$.

The structure functions F_1^H in the leading order accuracy are given by

$$2F_1^H(z,p_\perp;\mu^2)=\sum_q {e_q}^2[D_q^H(z,p_\perp;\mu^2)+D_{\bar{q}}^H(z,p_\perp;\mu^2)], \tag{4}$$

and F_L^H has not any term in the leading order. In this equation, the $D_q^H(z,p_\perp;\mu^2)$ is the ordinary unpolarized single-hadron FFs. In our analysis, we restrict ourselves to the leading order approximation in which the ${p_\perp}^2/\mu^2\ll 1$ limitation is applied. With these considerations, we may simply write the differential cross section formula as follows:

$$\frac{1}{\sigma_{\rm tot}}\frac{d\sigma^H}{dzd^2\vec{p}_\perp}=\frac{1}{\sum_q {e_q}^2}\sum_q {e_q}^2[D_q^H(z,p_\perp;\mu^2)+D_{\bar{q}}^H(z,p_\perp;\mu^2)]. \tag{5}$$

After integrating Eq. (5) over z and also considering $d^2\vec{p}_\perp=2\pi p_\perp dp_\perp$, we have the final formula for the differential cross sections in the leading order (LO) with respect to $p_\perp$:

$$\frac{1}{\sigma_{\rm tot}}\frac{d\sigma^H}{dp_\perp}=2\pi p_\perp\frac{1}{\sum_q {e_q}^2}\int\sum_q {e_q}^2[D_q^H(z,p_\perp;\mu^2)+D_{\bar{q}}^H(z,p_\perp;\mu^2)]dz, \tag{6}$$

and

$$\frac{1}{\sigma_{\rm tot}}\frac{d\sigma^H}{dz}=2\pi\frac{1}{\sum_q {e_q}^2}\int\sum_q {e_q}^2[D_q^H(z,p_\perp;\mu^2)+D_{\bar{q}}^H(z,p_\perp;\mu^2)]p_\perp dp_\perp. \tag{7}$$

B. The KMR and MRW prescriptions, UPDFs and UFFs

In the KMR [8] method, by starting from the DGLAP evolution equation and performing k_t factorization prescriptions, we obtain the UPDF of each parton which depends on the transverse momentum k_t, the fractional momentum x at hard scale μ^2 as

$$f_a(x,k_t,\mu^2)=T_a(k_t,\mu^2)\sum_b\left[\frac{\alpha_S(k_t^2)}{2\pi}\int_x^{1-\Delta}dzP_{ab}^{(0)}(z)b\left(\frac{x}{z},k_t^2\right)\right], \tag{8}$$

where the familiar double logarithmic Sudakov survival factor $T_a(k_t,\mu^2)$ is

$$T_a(k_t,\mu^2)=\exp\left(-\int_{k_t^2}^{\mu^2}\frac{\alpha_S(\kappa_t^2)}{2\pi}\frac{d\kappa_t^2}{\kappa_t^2}\sum_b\int_0^{1-\Delta'}dz'P_{ba}^{(0)}(z')\right), \tag{9}$$

where $P_{ab}^{(0)}(z)$ ($b=q,\bar{q}$ and g) denotes the usual LO splitting functions and $b(\frac{x}{z},k_t^2)$ are the LO PDFs (the Sudakov form factor becomes the equal one for $k_t>\mu$). In this formula, the angular-ordering constraint (AOC) [50–56], Δ (Δ'), is applied in the upper limit of the integration, which is an infrared cutoff to prevent the soft gluon singularities from rising from the splitting functions and defined as $\Delta=\frac{k_t}{\mu+k_t}$ ($\Delta'=\frac{\kappa_t}{\mu+\kappa_t}$), which constrains the k_t ordering.

Similarly, we can obtain a formula for the quark UFFs by starting from the complete (leading order) DGLAP evolution equation for the quark FFs in terms of quark and gluons, see Fig. 1 (a similar equation can be written for the antiquarks, throughout this report):

$$\frac{\partial D_q^H(z,\mu^2)}{\partial ln\mu^2}=\frac{\alpha_S(\mu^2)}{2\pi}\int_x^1\frac{dx}{x}\left[P_{qq}(x)D_q^H\left(\frac{z}{x},\mu^2\right)+P_{gq}(x)D_g^H\left(\frac{z}{x},\mu^2\right)\right]. \tag{10}$$

Note that in this formula, according to Refs. [15,19], the functions P_{gq} are interchanged in comparison with that of parton evolution equations. The relevant splitting kernels are

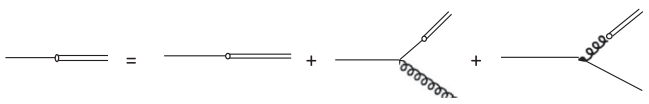

FIG. 1. The graphical representation of Eq. (10).

$$P_{qq}(x) = C_F\left[\frac{1+x^2}{(1-x)_+} + \frac{3}{2}\delta(1-x)\right], \tag{11}$$

$$P_{gq}(x) = C_F\frac{1+(1-x^2)}{x}. \tag{12}$$

By inserting these splitting kernels and using the *plus* prescription in a straightforward way, one could have the LO DGLAP equation evaluated at a scale k_t:

$$\frac{\partial \mathcal{D}_q^H(z,k_t^2)}{\partial ln k_t^2} = \frac{\alpha_S(k_t^2)}{2\pi}\left\{\sum_a \int_z^{1-\Delta} P_{aq}(x)\mathcal{D}_a^H\left(\frac{z}{x},k_t^2\right)dx - \mathcal{D}_q^H(z,k_t^2)\sum_a \int_x^{1-\Delta} P_{qa}(z')dz'\right\}. \tag{13}$$

Here, P_{aq} refer to the unregulated LO DGLAP splitting kernels and $\mathcal{D}_i^H(z,k_t^2) = zD_i^H(z,k_t^2)$ ($i = q,\bar{q}$ and g). The two terms on the right-hand side correspond to real and virtual emission, respectively. The virtual contributions may be resummed to all orders by the Sudakov form factor,

$$T_q(k_t,\mu^2) = \exp\left(-\int_{k_t^2}^{\mu^2}\frac{\alpha_S(\kappa_t^2)}{2\pi}\frac{d\kappa_t^2}{\kappa_t^2}\sum_b\int_0^{1-\Delta}dz' P_{qb}^{(0)}(z')\right), \tag{14}$$

which is the survival probability that hadron H with transverse momentum k_t remains untouched in the evolution, up to the factorization scale μ. Therefore, the UFFs become dependent on the two scales, k_t^2 and μ^2 in the *last step* of the evolution. So, in the k_t-factorization framework, the UFFs have the following forms:

$$D_q^H(z,k_t,\mu^2) = T_q(k_t,\mu^2)\sum_{b=q,g}\left[\frac{\alpha_S(k_t^2)}{2\pi k_t^2}\int_z^{1-\Delta}dz' P_{bq}^{(0)}(z')\mathcal{D}_b^H\left(\frac{z}{z'},k_t^2\right)\right], \tag{15}$$

where $\mathcal{D}_b^H(\frac{z}{z'},k_t^2)$ are the collinear, unpolarized quarks and gluons FFs. We use the LO set of DSS [57]. Note that in general we set $k_t = p_\perp/z$ [31] for the UFFs to calculate different differential cross sections.

By applying the AOC only on the terms which include the on shell gluon emissions for the quarks and gluons, we have the LO-MRW UFFs for quarks in the following form:

$$D_q^{H,LO}(z,k_t,\mu^2) = T_q(k_t,\mu^2)\frac{\alpha_S(k_t^2)}{2\pi k_t^2}\int_z^1 dz'\left[P_{qq}^{(0)}(z')\frac{z}{z'}D_q^H\left(\frac{z}{z'},k_t^2\right)\Theta\left(\frac{\mu}{\mu+k_t}-z'\right) + P_{gq}^{(0)}(z')\frac{z}{z'}D_g\left(\frac{z}{z'},k_t^2\right)\right], \tag{16}$$

with

$$T_q(k_t,\mu^2) = \exp\left(-\int_{k_t^2}^{\mu^2}\frac{\alpha_S(\kappa_t^2)}{2\pi}\frac{d\kappa_t^2}{\kappa_t^2}\sum_b\int_0^{1-\Delta}dz' P_{qb}^{(0)}(z')\right). \tag{17}$$

By expanding the MRW formalism to the NLO level, we have

$$D_q^{H,NLO}(z,k_t,\mu^2) = \int_z^1 dz' T_q(k,\mu^2)\frac{\alpha_S(k^2)}{2\pi k_t^2}\sum_{b=q,\bar{q},g}\tilde{P}_{bq}^{(0+1)}(z')\,D_b^{H,NLO}\left(\frac{z}{z'},k^2\right)\Theta\left(1-z'-\frac{k_t^2}{\mu^2}\right), \tag{18}$$

where $k^2 = \frac{k_t^2}{(1-z')}$. In the above formula, the Sudakov form factor is defined as

$$T_q(k,\mu^2) = \exp\left(-\int_{k^2}^{\mu^2}\frac{\alpha_S(\kappa_t^2)}{2\pi}\frac{d\kappa_t^2}{\kappa_t^2}\int_0^1 dz' z'[\tilde{P}_{qq}^{(0+1)}(z') + \tilde{P}_{qg}^{(0+1)}(z')]\right), \tag{19}$$

The higher order splitting functions are presented in the Appendix.

III. NUMERICAL RESULTS AND DISCUSSIONS

In this section, we intend to present the kinematic and theoretical aspects of our calculations. First, we calculate the KMR UFF based on the k_t-factorization scheme by applying exactly analogous steps hold for the UPDF [8] which was developed in Sec. II. The similar perturbative calculation for both LO-MRW and NLO-MRW FF are also implemented. It is important, however, to point out that the crucial constraint for instructing any new UFF is the normalization relation,

$$D_q^H(z,\mu^2) \simeq \int^{\mu^2} dp_\perp^2 D_q^H(z,p_\perp,\mu^2). \tag{20}$$

In this article, we attempt to extract information about the perturbative evolution region. So, we restrict our analysis to the region of $p_\perp > 1.0$ GeV. Moreover, we vary the scale μ between $\mu/2$ and 2μ to assess the uncertainty in the perturbative calculation.

The results of the above numerical calculations are compared with the available experimental datasets of the single inclusive hadron production in the e^+e^- annihilation processes of the TASSO detector at PETRA (DESY) [35,36] laboratories and the Belle detector at the KEKB [44]. We use the data from different groups such as the AMY, MARK II, and CELLO collaborations. The results are demonstrated in Figs. 2–6 and compared with the different collaborations data at different c.m. energies. In Figs. 2–4, the numerical results related to the UFF are shown by the solid, dash, and dot-dashed curves and correspond to the result of different schemes, namely the KMR, LO-MRW, and NLO-MRW, respectively.

We start by analyzing the cross sections related to the low c.m. energies for $\sqrt{s} = 14$, 22, 35 and 44 GeV. The results of the normalized differential cross sections $(1/\sigma_{\rm tot})d\sigma/dp_\perp$ with respect to $p_\perp$ are compared to the experimental data of TASSO at the different c.m. energies which are shown in Fig. 2. It is demonstrated that as the c.m. energy is increased the differential cross sections evaluated by using the three UFFs schemes, become near to each other, especially in the case of KMR and LO-MRW formalisms. On the other hand, our results become closer to the data for the lower values of $p_\perp$ and the higher values of c.m. energies.

In Fig. 3(a), the normalized distribution of the multiplicity with respect to $p_\perp$ for charged particles,

$$\frac{1}{N}\frac{dN}{dp_\perp} = 2\pi p_\perp \frac{1}{\sum_q {e_q}^2}\int \sum_q {e_q}^2 [D_q^H(z,p_\perp;\mu^2) + D_{\bar{q}}^H(z,p_\perp;\mu^2)]dz, \tag{21}$$

is compared to the experimental data of CELLO [39] while in panels (b)–(d), the normalized differential cross sections with respect to $p_\perp^2$ are compared to the experimental data of TASSO [36] at the different c.m. energies. The same conclusion can be made for this figure as the one we made for Fig. 2. It is also observed that the KMR and NLO-MRW are closer to each other.

In Fig. 4, the normalized differential cross sections with respect to $p_\perp$ for charged particles is compared to the experimental data of AMY [38] [panel (a)], and

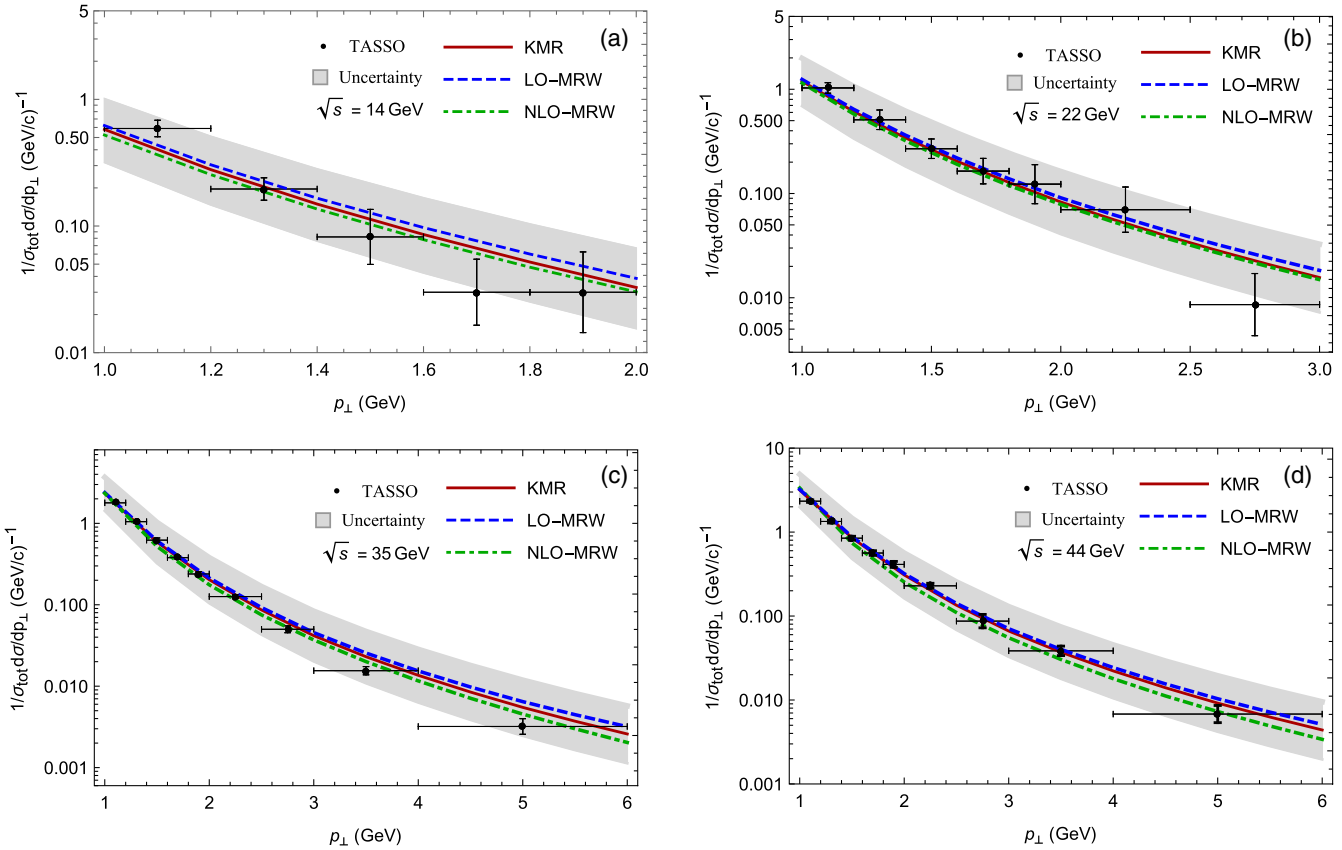

FIG. 2. The normalized differential cross sections $(1/\sigma_{\rm tot})d\sigma/dp_\perp$ with respect to $p_\perp$ compared to the experimental data of TASSO [36] at the different c.m. energies. The shaded uncertainty gray bands belong to the KMR prescription.

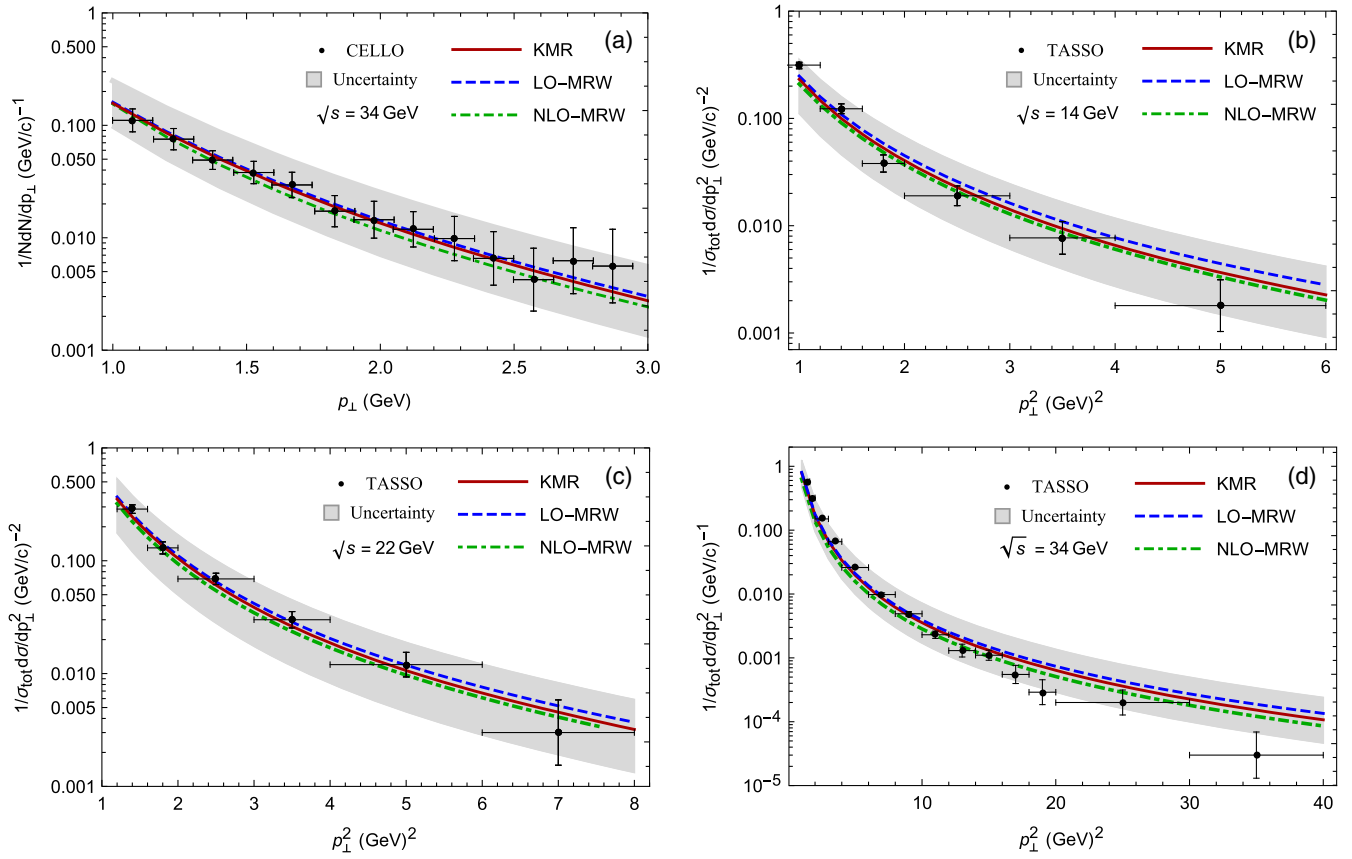

FIG. 3. (a) The normalized distribution of the multiplicity with respect to $p_\perp$ for charged particles is compared to the experimental data of CELLO [39]. (b)–(d) The normalized differential cross sections with respect to $p_\perp$ compared to the experimental data of TASSO [36] at the different c.m. energies. The shaded uncertainty gray bands belong to the KMR prescription.

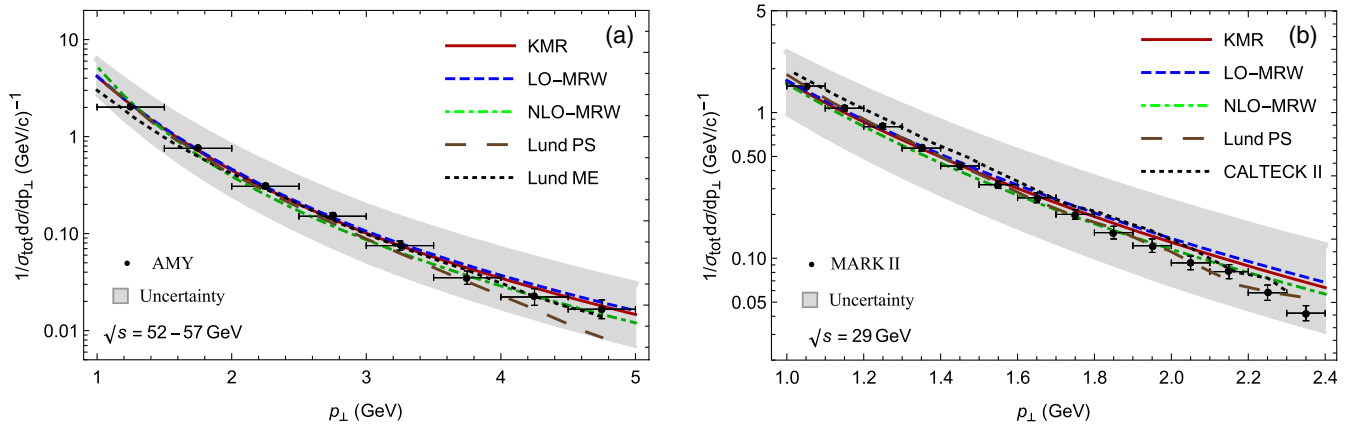

FIG. 4. The normalized differential cross sections with respect to $p_\perp$ for charged particles is compared to the experimental data of AMY [38] (the left panel), of MARK II [37] (the right panel), and some "QCD + fragmentation" models predictions. The shaded uncertainty gray bands belong to the KMR prescription.

MARK II [37] [panel (b)]. A comparison between our results and some Monte Carlo techniques, i.e., the Lund parton shower (Lund PS) (the dashed lines in both panels), the Lund matrix elements (Lund ME) [the dotted line in panel (a)] and the CALTECH II [the dotted line in panel (b)] models are presented. It is observed that our results are similar to those of QCD + fragmentation function models. It seems that the Lund parton shower model provides a better description of data, since according to Ref. [38], the total χ^2 of the fits following this approach is the lowest among the three models. However, the advantage of the k_t-factorization methodology is that the calculation is

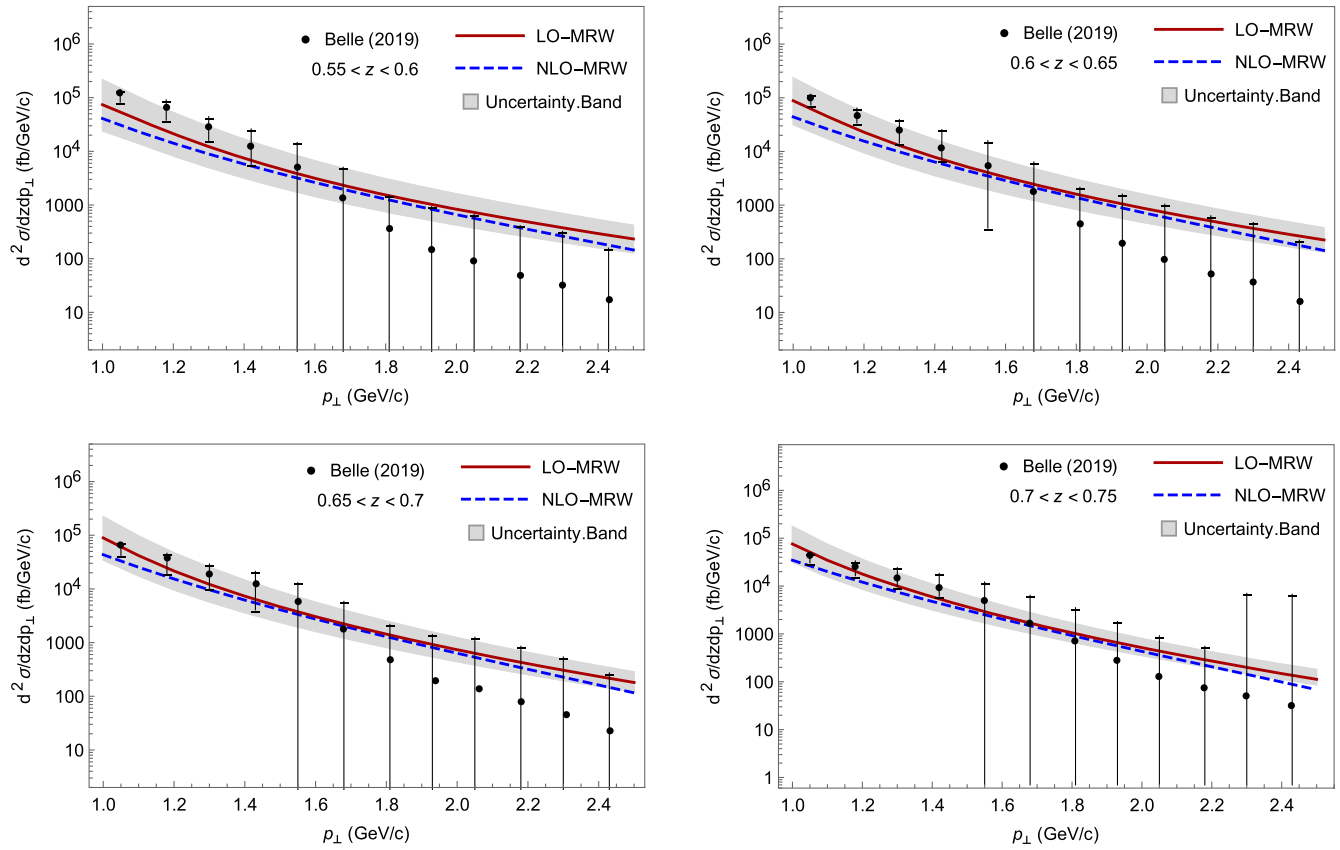

FIG. 5. The differential cross sections for pions as a function of $p_\perp$ for the indicated z bins and thrust $0.85 < T < 0.9$. The error gray bands represent the uncertainties for LO-MRW formalism. The results are compared to the experimental data of the Belle collaboration [44] in the $\sqrt{s} = 10.58$ GeV center of mass energy.

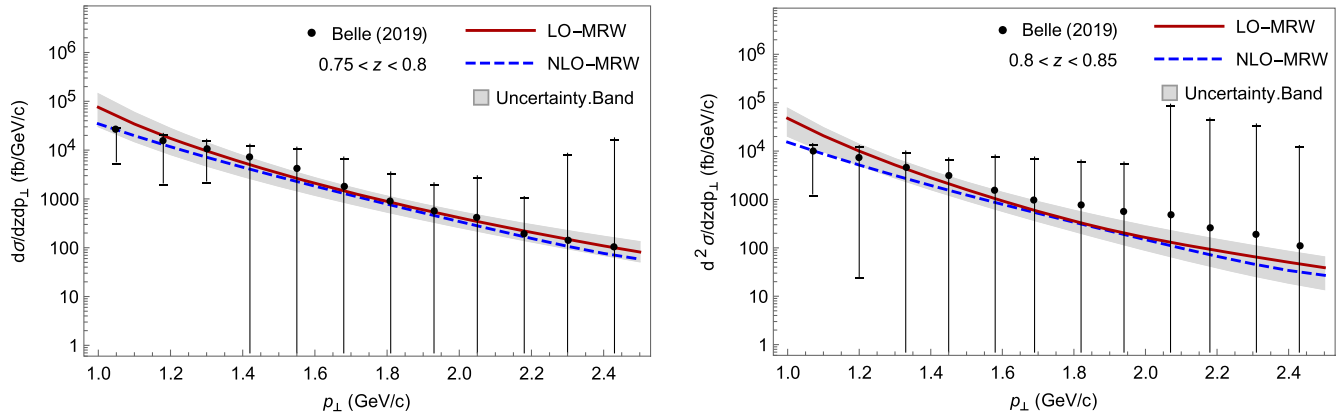

FIG. 6. The same as Fig. 5.

completely perturbative and we do not use any fitting procedure to have a prediction of the data.

In Figs. 5 and 6, our results of LO- and NLO-MRW are compared with the differential cross section datasets of pions from the Belle collaboration [44] as a function of transverse momentum $p_\perp$ for the indicated z bins and thrust value $0.85 < T < 0.9$. These figures show as the amount of z bin increases, the result of NLO-MRW scheme becomes closer to the data.

As we pointed out before, it is obvious that all three approaches have similar behavior. Although near $p_\perp \sim 1$, there is not any significant preference between the results of three schemes, but by increasing $p_\perp$ they start to separate from each other. According to these panels, our results show a bit underestimate and overestimate in the low and high $p_\perp$ region. However, the uncertainty bands of our calculations cover the experimental data. Thus, one can conclude that our perturbative and straightforward

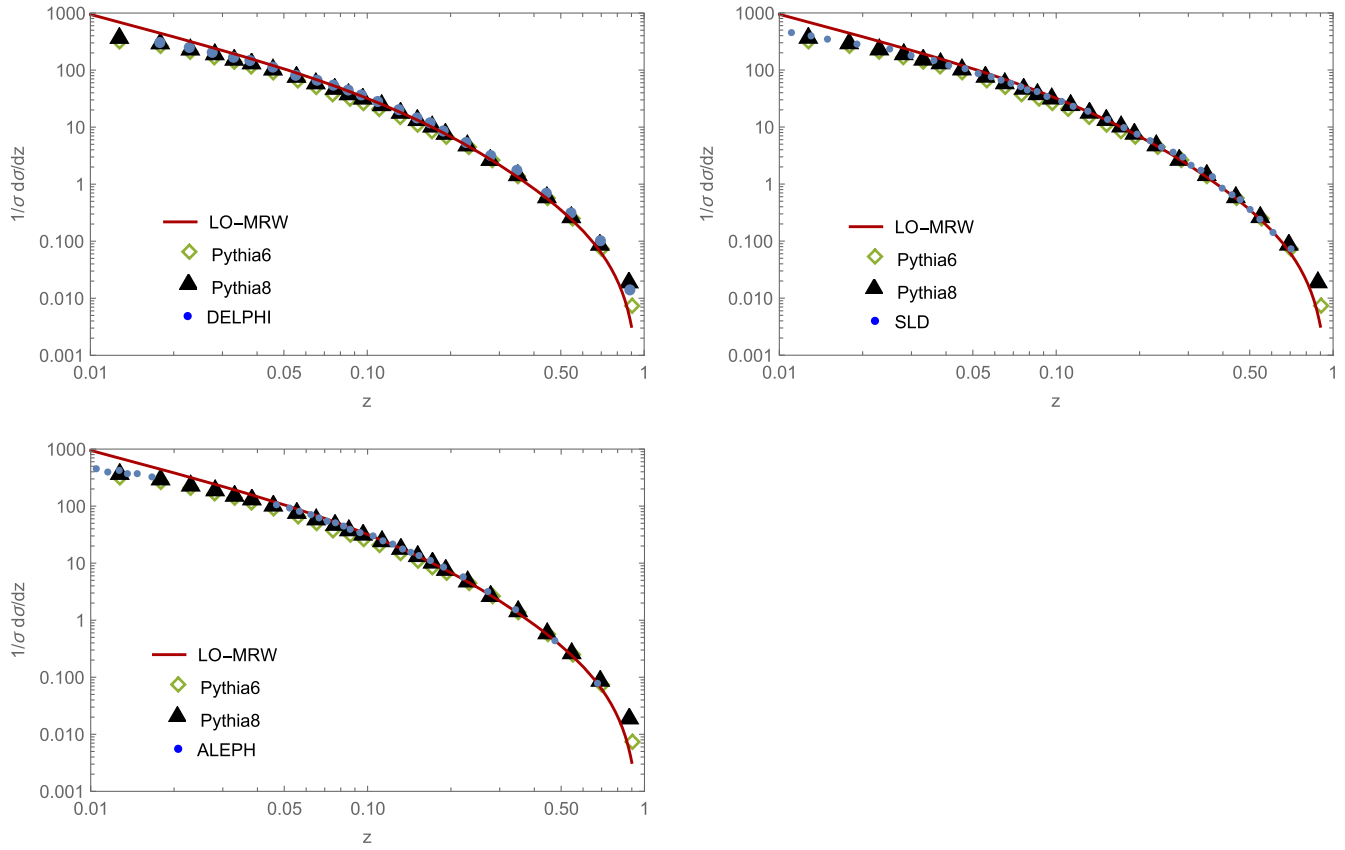

FIG. 7. The comparison of our differential cross section defined in Eq. (7), using the LO-MRW formalism, with those of PYTHIA6.4 and PYTHIA8.2 parton showers [40] as well as the DELPHI [41], SLD [42] and ALEPH [43] collaborations data, at c.m. energy 91 GeV.

calculations (using the KMR and MRW methods) give a good description of the data.

In different panels of Fig. 7, we compare our differential cross section defined in Eq. (7), using the LO-MRW formalism, with those of new PYTHIA6.4 and PYTHIA8.2 parton showers [40] as well as the DELPHI [41], SLD [42] and ALEPH [43] collaboration data, at c.m. energy 91 GeV. There is good agreement between our prediction and the mentioned experimental data as well as new parton showers, especially for the PYTHIA8.2 parton shower [40].

IV. CONCLUSIONS

We presented the first analysis of the applicability of the k_t-factorization approach in the single inclusive hadron production in the e^+e^- annihilation processes. We used the transverse momentum dependent fragmentation functions of three different prescriptions, i.e., KMR, MRW, and NLO-MRW. We calculated several distributions of normalized transverse momentum and multiplicity of the charged fragmented hadrons in the leading order. In addition, we obtained the uncertainty band for the cross section distribution in the case of KMR by changing the scale factor as illustrated in Sec. III. We found with a good approximation, all three schemes give a similar and acceptable description of data presented in this report.

In Ref. [58] the transverse-momentum-dependent FFs (or UFFs) up to N3LO QCD were calculated. However, it is the first time that present formalism is applied to calculate the unintegrated fragmentation functions up to the NLO level and should be considered as the first step for application of KMR and MRW formalisms. On the other hand, we only considered the lowest order structure functions for the evaluation of differential cross sections. So, we hope by extending our formalism to the next-leading order in the structure functions and improving of the UFFs, we could get better accuracy, in the future works.

ACKNOWLEDGMENTS

M. Modarres and R. Taghavi would like to acknowledge the research support of the University of Tehran and the Iran National Science Foundation (INSF) for their grants.

APPENDIX: THE NLO SPLITTING FUNCTIONS

The NLO splitting functions are defined as [59]

$$\tilde{P}_{ab}^{(0+1)}(z) = \tilde{P}_{ab}^{(0)}(z) + \frac{\alpha_S}{2\pi}\tilde{P}_{ab}^{(1)}(z), \tag{A1}$$

with

$$\tilde{P}_{ab}^{(i)}(z) = P_{ab}^{(i)}(z) - \Theta(z-(1-\Delta))\delta_{ab}F_{ab}^{(i)}P_{ab}(z), \quad \text{(A2)}$$

where $i = 0$ and 1 stand for the LO and the NLO, respectively. Δ can be defined as [9]

$$\Delta = \frac{\kappa_t\sqrt{1-z}}{\kappa_t\sqrt{1-z}+\mu},$$

and we have

$$F_{qq}^{(0)} = C_F, \quad \text{(A3)}$$

$$F_{qq}^{(1)} = -C_F\left(T_R N_F\frac{10}{9} + C_A\left(\frac{\pi^2}{6}-\frac{67}{18}\right)\right), \quad \text{(A4)}$$

$$F_{gg}^{(0)} = 2C_A, \quad \text{(A5)}$$

$$F_{gg}^{(1)} = -2C_F\left(T_R N_F\frac{10}{9} + C_A\left(\frac{\pi^2}{6}-\frac{67}{18}\right)\right), \quad \text{(A6)}$$

$$P_{qq}(z) = \frac{(1-z^2)}{1-z}, \quad \text{(A7)}$$

$$P_{gg}(z) = \frac{z}{(1-z)} + \frac{(1-z)}{z} + z(1-z). \quad \text{(A8)}$$

[1] V. N. Gribov and L. N. Lipatov, Yad. Fiz. **15**, 781 (1972).
[2] L. N. Lipatov, Sov. J. Nucl. Phys. **20**, 94 (1975).
[3] G. Altarelli and G. Parisi, Nucl. Phys. **B126**, 298 (1977).
[4] Y. L. Dokshitzer, Sov. Phys. JETP **46**, 641 (1977).
[5] S. M. Aybat and T. C. Rogers, Phys. Rev. D **83**, 114042 (2011).
[6] Mengyun Liu and Bo-Qiang Ma, Phys. Rev. D **98**, 036024 (2018).
[7] R. Taghavi and M. Mirjalili, Mod. Phys. Lett. A **32**, 1750040 (2017).
[8] M. A. Kimber, A. D. Martin, and M. G. Ryskin, Phys. Rev. D **63**, 114027 (2001).
[9] A. D. Martin, M. G. Ryskin, and G. Watt, Eur. Phys. J. C **66**, 163 (2010).
[10] M. Modarres, H. Hosseinkhani, and N. Olanj, Nucl. Phys. **A902**, 21 (2013).
[11] M. Modarres and H. Hosseinkhani, Few-Body Syst. **47**, 237 (2010).
[12] M. Modarres and H. Hosseinkhani, Nucl. Phys. **A815**, 40 (2009).
[13] H. Hosseinkhani and M. Modarres, Phys. Lett. B **694**, 355 (2011).
[14] H. Hosseinkhani and M. Modarres, Phys. Lett. B **708**, 75 (2012).
[15] J. F. Qwens, Phys. Lett. B **76**, 1 (1978).
[16] J. F. Owens, Phys. Rev. D **20**, 221 (1979).
[17] J. F. Owens, Rev. Mod. Phys. **59**, 465 (1987).
[18] S. Albino, Rev. Mod. Phys. **82**, 2489 (2010).
[19] A. Metz and A. Vossen, Prog. Part. Nucl. Phys. **91**, 136 (2016).
[20] J. C. Collins and D. E. Soper, Nucl. Phys. **B194**, 445 (1982).
[21] J. P. Lees *et al.* (*BABAR* Collaboration), Phys. Rev. D **90**, 052003 (2014).
[22] J. P. Lees *et al.* (*BABAR* Collaboration), Phys. Rev. D **92**, 111101 (2015).
[23] Z.-B. Kang, A. Prokudin, P. Sun, and F. Yuan, Phys. Rev. D **91**, 071501 (2015).
[24] A. Bacchetta, M. G. Echevarria, P. J. G. Mulders, M. Radici, and A. Signori, J. High Energy Phys. 11 (2015) 076.
[25] M. Anselmino, M. Boglione, U. DAlesio, J. O. Gonzalez Hernandez, S. Melis, F. Murgia, and A. Prokudin, Phys. Rev. D **93**, 034025 (2016).
[26] A. Signori, A. Bacchetta, M. Radici, and G. Schnell, J. High Energy Phys. 11 (2013) 194.
[27] M. Anselmino, M. Boglione, J. Gonzalez Hernandez, S. Melis, and A. Prokudin, J. High Energy Phys. 04 (2014) 005.
[28] C. A. Aidala, B. Field, L. P. Gamberg, and T. C. Rogers, Phys. Rev. D **89**, 094002 (2014).
[29] J. Collins, L. Gamberg, A. Prokudin, T. C. Rogers, N. Sato, and B. Wang, Phys. Rev. D **94**, 034014 (2016).
[30] M. Boglione, J. Collins, L. Gamberg, J. O. Gonzalez-Hernandez, T. C. Rogers, and N. Sato, Phys. Lett. B **766**, 245 (2017).
[31] M. Boglione, J. O. Gonzalez-Hernandez, and R. Taghavi, Phys. Lett. B **772**, 78 (2017).
[32] A. Bacchetta, F. Delcarro, C. Pisano, M. Radicib, and A. Signoric, J. High Energy Phys. 06 (2017) 081.
[33] Z.-B. Kang, D. Yu Shaoa, and F. Zhaoa, J. High Energy Phys. 12 (2020) 127.
[34] R. Seidl *et al.* (Belle Collaboration), Phys. Rev. D **99**, 112006 (2019).
[35] M. Althoff *et al.*, Z. Phys. C **22**, 307 (1984).
[36] W. Braunschweig *et al.*, Z. Phys. C **47**, 187 (1990).
[37] A. Petersen *et al.*, Phys. Rev. D **37**, 1 (1988).
[38] Y. K. Li *et al.* (AMY Collaboration), Phys. Rev. D **41**, 9 (1990).
[39] H. J. Behrend *et al.* (CELLO Collaboration), Z. Phys. C **14**, 189 (1982).
[40] H. Bello Martnez, R. J. Hernndez-Pinto, and I. Len Monzn, in *Proceedings of the 7th Annual Conference on Large*

Hadron Collider Physics—LHCP2019 (Proceedings of Science, Mexico, 2019).
[41] P. Abreu *et al.* (DELPHI Collaboration), Eur. Phys. J. C **5**, 585 (1998).
[42] K. Abe *et al.* (SLD Collaboration), Phys. Rev. D **59**, 052001 (1999).
[43] D. Buskulic *et al.* (ALEPH Collaboration), Z. Phys. C **66**, 355 (1995).
[44] R. Seidl *et al.* (Belle Collaboration), Phys. Rev. D **99**, 112006 (2019).
[45] T. Sjostrand and M. Bengtsson, Comput. Phys. Commun. **43**, 367 (1987).
[46] F. Gutbord, G. Kramer, and G. Schierholz, Z. Phys. C **21**, 235 (1984).
[47] T. D. Gottschalk and D. Morris, Nucl. Phys. **B288**, 729 (1987).
[48] G. Altarelli, Phys. Rep. **81**, 1 (1982).
[49] D. Florian, M. Stratmann, and W. Vogelsang, Phys. Rev. D **57**, 5811 (1998).
[50] M. Ciafaloni, Nucl. Phys. **B296**, 49 (1988).
[51] S. Catani, F. Fiorani, and G. Marchesini, Phys. Lett. B **234**, 339 (1990).
[52] S. Catani, F. Fiorani, and G. Marchesini, Nucl. Phys. **B336**, 18 (1990).
[53] M. G. Marchesini, in *Proceedings of the Workshop QCD at 200 TeV Erice, Italy*, edited by L. Cifarelli and Yu. L. Dokshitzer (Plenum, New York, 1992), p. 183.
[54] G. Marchesini, Nucl. Phys. **B445**, 49 (1995).
[55] G. Marchesini and B. R. Webber, Nucl. Phys. **B310**, 461 (1988).
[56] Y. L. Dokshitzer, V. A. Khoze, S. I. Troyan, and A. H. Mueller, Rev. Mod. Phys. **60**, 373 (1988).
[57] D. de Florian, R. Sassot, and M. Stratmann, Phys. Rev. D **76**, 074033 (2007).
[58] M.-x. Luo, T.-Z. Yang, H. X. Zhua, and Y. J. Zhua, J. High Energy Phys. 06 (2021) 115.
[59] W. Furmanski and R. Petronzio, Phys. Lett. **97B**, 437 (1980).